Journal of Medical Systems (2019) 43: 326
https://doi.org/10.1007/s10916-019-1453-8

IMAGE & SIGNAL PROCESSING

A New Approach for Brain Tumor Segmentation and Classification Based on Score Level Fusion Using Transfer Learning

Javeria Amin[1,2] · Muhammad Sharif[2] · Mussarat Yasmin[2] · Tanzila Saba[3] · Muhammad Almas Anjum[4] · Steven Lawrence Fernandes[5]

Received: 18 February 2019 / Accepted: 4 September 2019 / Published online: 23 October 2019

Abstract
Brain tumor is one of the most death defying diseases nowadays. The tumor contains a cluster of abnormal cells grouped around the inner portion of human brain. It affects the brain by squeezing/ damaging healthy tissues. It also amplifies intra cranial pressure and as a result tumor cells growth increases rapidly which may lead to death. It is, therefore desirable to diagnose/ detect brain tumor at an early stage that may increase the patient survival rate. The major objective of this research work is to present a new technique for the detection of tumor. The proposed architecture accurately segments and classifies the benign and malignant tumor cases. Different spatial domain methods are applied to enhance and accurately segment the input images. Moreover Alex and Google networks are utilized for classification in which two score vectors are obtained after the softmax layer. Further, both score vectors are fused and supplied to multiple classifiers along with softmax layer. Evaluation of proposed model is done on top medical image computing and computer-assisted intervention (MICCAI) challenge datasets i.e., multimodal brain tumor segmentation (BRATS) 2013, 2014, 2015, 2016 and ischemic stroke lesion segmentation (ISLES) 2018 respectively.

Keywords Brain tumor detection · Alex network · Google network · Fused score vector · Softmax layer · Segmentation · Classification

Introduction

Gliomas are primary type of brain tumors which originate from the glial cells and approximately 70% adults are suffering from this type of disease. The tumor cells grow rapidly and might be characterized into two grades i.e., low grade (oligodendroglioma) and high grade (glioblastoma) [1]. When tumor cells are diagnosed/ detected at an early stage, they are less lethal as compared to final stage which reduces the patient survival rate in less than two years. Chemotherapy, therapy, surgery or combinations of these are most common treatment for tumor patients. Due to high multi planar MR image resolution, magnetic resonance imaging (MRI) is primarily utilized

This article is part of the Topical Collection on *Image & Signal Processing*

✉ Javeria Amin
javeria.amin@uow.edu.pk

Muhammad Sharif
muhammadsharifmalik@yahoo.com

Mussarat Yasmin
mussarat@ciitwah.edu.pk

Tanzila Saba
tsaba@psu.edu.sa

Muhammad Almas Anjum
almananjum@yahoo.com

Steven Lawrence Fernandes
steven.ec@sahyadri.edu.in

[1] Department of Computer Science, University of Wah, Wah, Pakistan

[2] Department of Computer Science, COMSATS University Islamabad, Wah Campus Pakistan, Wah, Pakistan

[3] College of Computer and Information Sciences, Prince Sultan University, Riyadh 11586, Saudi Arabia

[4] College of EME, NUST Pakistan, Islamabad, Pakistan

[5] Department of Electronics and Communication Engineering, Sahyadri College of Engineering & Management, Mangaluru, India

for gliomas detection [2]. The MR image segmentation [3] is a crucial task to monitor the variation in volume of tumors. It plays vital role in radiotherapy/ surgical planning where affected/ healthy regions are clearly segregated [4, 5]. Presently, the performance of manual segmentation is more dominative in the clinical routine where more clinical practice and time is required by the radiologists. Moreover, complex glioma features and subtle variations among MRI analysis also generate inescapable challenges for reliable detection through visual examination of MRI even through expert radiologist. Automatic approaches for the detection of brain tumor are more noteworthy and meaningful. Segmentation approaches for brain tumor using 2D slices of MRI are divided into three classes i.e., threshold, region based and pixel based classification [6]. Threshold approaches do not provide <1 threshold to classify the target voxel segmentation through their intensities. Sobel filter is employed to outline the edges of voxels. Then pixel values of each voxel are compared with threshold criteria and every pixel value is assigned to adjacent regions to refine the output. Region based techniques isolate the voxels manually into exclusive districts [7]. It is a classical method in which one seed is at least planted in each district and each voxel similarity with the adjacent seeds is measured [8]. This method might not address the partial volume effect. A modified technique is presented which reduces the partial volume effect and detects more refined edges of voxels through computation of gradient information [9]. The adaptive region growing [10, 11] techniques are used to precise segmentation of tumor region [12]. Pixel based classification techniques using multi sequence (T1C, T2, Flair and T1) are divided into each voxel i.e., supervised, unsupervised and semi-supervised. In unsupervised approaches, clusters are made by measuring similarity on the basis of angular discrepancy and feature distance of each voxel [13]. Markov random field (MRF) is a semi-supervised method to minimize the problems including overlapping region and noisy voxels [14]. Multi-layer MRF method is employed for the detection of brain tumor. This method focuses on different information related to intensity i.e., intra/ inter structure properties and neighborhood coherence. The spatial accuracy weighted HMRF and expectation maximization (EM) methods are used to overcome the anisotropic issues created through different MRI resolution [15]. Conditional random field (CRF) model is utilized for tumor detection in less processing time [16]. Convolutional neural networks (CNN) approaches are used as supervised classification where different information is segmented with no requirement of distributed parametric hypothesis [17]. Deep neural architecture is applied to extract the discriminative features [18]. Image net recognition through deep model of CNN is used to segment the brain tumor [19]. Patch based CNN architecture is utilized to classify the healthy/ unhealthy voxels [20]. Cascaded CNN architecture is employed for the detection of tumor voxels [21]. The CNN methods are applied with small convolutional kernel for the segmentation of MRI [22]. Hybrid approach (clustering and CNN) is used to analyze MR images [23]. Eleven layer 3D CNN architecture is employed for the classification of healthy/ unhealthy tissues in MRI [24].

Contribution

The proposed method major contribution is described as follows.

1. Input images are converted into single channel and then linear/ log transformation with convolution window size is applied to smooth image intensity values. Moreover, a global threshold and morphological operation are applied to segment the brain tumor more accurately.
2. In the classification phase, a new approach is presented to classify the tumor/non-tumor MR images in which segmented images are supplied to pre-train CNN model in which feature learning is performed through Alex net and Google net. Fully connected layer is used for feature mapping and score vector is obtained from each training model. Then score vectors obtained after the softmax layer are fused. Moreover, fused vector is supplied to the softmax layer as well as multiple classifiers.

Related work

Several CNNs architecture are presented in literature for tumor detection [25]. These architectures have rapidly designed from prediction on single label to dense schemes such as U-Net [26] and DeepMedic [27] architecture. The Hyper column model is applied to extract information from CNN architecture [28]. Moreover, U-net and its modified techniques are a vital series of architecture to segment the medical images [29]. They contain encoding/ decoding model with down-sampling/ up-sampling operations. U-net model presents feature mapping in encoding to decoding model by performing successive concatenation [30]. Several methods are presented in literature but still no existing method achieves better results in all performance metrics. The proposed model obtained good results in terms of all performance measures on five challenging datasets. This study investigates a new score level fusion approach for the detection of glioma and stroke [31] lesions accurately using computed tomography (CT) as well as MRI.

Proposed approach

The presented methodology having four major steps as normalization, segmentation and classification with fusing score of Alex/ Google deep learning model using MRI/ CT modalities is presented in Fig. 1.

Lesion enhancement

MRI and CT have different intensity values that are affected through bias field. Hence a more robust method is proposed to normalize the image intensity values that provide better segmentation results. The input images are resized with 256 and converted into single channel 256 because color image intensities are transformed into single channel for fast processing. Image enhancement is a more vital step in preprocessing because it provides better contrast and information when compared with non-enhanced input images. In this process, each input image values are subtracted from ∂-1 that is mapped into resultant image ($\propto = (\partial - 1) - \rho$). Number of gray levels in input images are 256 ($\propto = 255 - \rho$)in which each value of input image is subtracted from 255. Here, lighter/ darker pixel values are transformed into darker/ lighter regions. Moreover, log transformation ($\propto = k \log(\rho + 1)$), where k = 1 is applied to adjust required enhancement as shown in Fig. 2.

Lesion segmentation

The segmentation is performed individually across each input image. The input image contains 0–255 pixel level values. Thresholding is a more accurate technique to segment the actual lesion symptom on pixel intensity values. Therefore, optimal threshold value is selected (T = 160) for segmentation.

$$S_i = \begin{cases} 1 & if\ S_i(Row, Col) > T \\ 0 & otherwise \end{cases} \quad (1)$$

The resultant image (S_i) in eq. (1) is not refined enough. Therefore, 4 disc shape structuring element is applied to extract actual tumor pixels shown in Fig. 4.

$$\mathcal{R}(S_i) = \Psi(\lambda(S_i)) \quad (2)$$

Here, in eq. (2), $\mathcal{R}, \lambda, \Psi$ represent the opening, erosion and dilation operations in which 3 disk shape structuring element is used to fill near boundary holes as given in eq. (3). The tumor segmentation results are shown in Figs. 5 and 6.

$$f(x) = \begin{cases} 0 & x \in structuring\ element \\ -\infty & otherwise \end{cases} \quad (3)$$

Proposed CNN model

The segmented images are supplied for the classification of normal and healthy MR images. Pre-trained Alex net [32] and Google net [33] are fine tuned for discrimination purpose. Input images are divided into training and testing set and labeled to perform supervised learning. In training phase, input

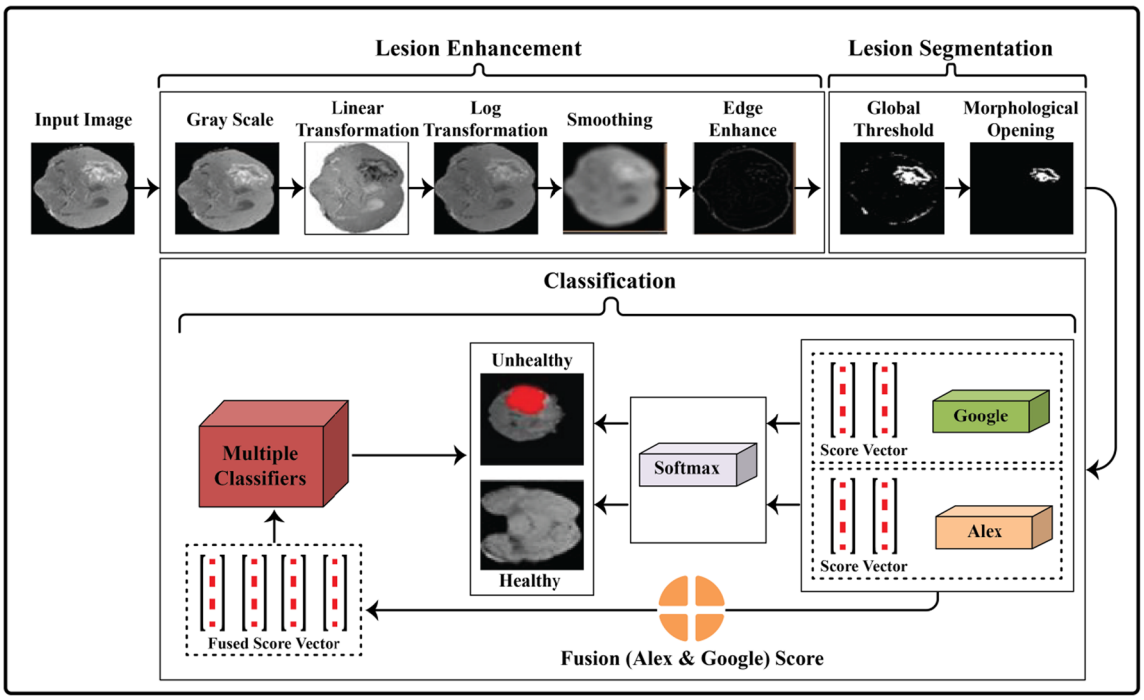

Fig. 1 Overview of proposed approach steps

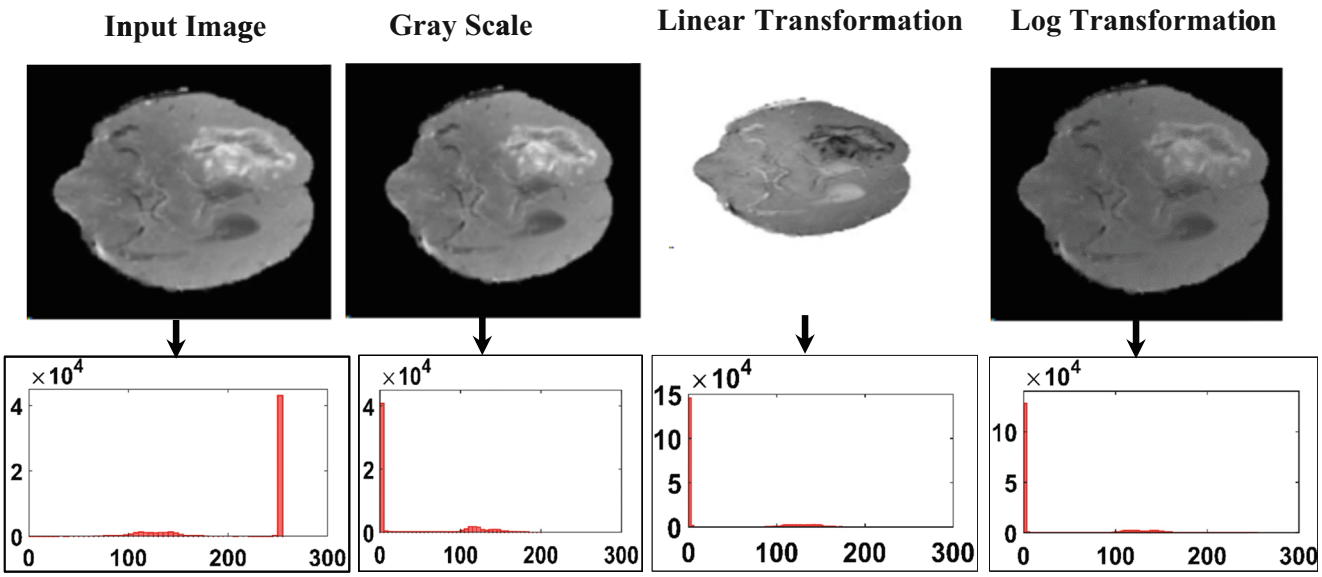

Fig. 2 Image enhancement

images are supplied to the proposed CNN model. In the same situation, testing is performed on the basis of training to measure the proposed method performance. The proposed model is depicted in a block diagram shown in Fig. 7.

The proposed model consists of hierarchical architecture containing different kinds of layers attached to each other. Each layer processes the input and output feature mapping. Moreover, including input layer, major layers that are utilized in proposed model are down-sampling, convolution, dropout, softmax, regularization and fully connected layers. In convolution layers, I denotes input vector at layer L (the dimension of each input vector is ($Row_L \times COL_L \times$ Gray channel (CC)) that is convolved through kernels bank (F) with dimension ($Row_F \times COL_F \times$ Color channel (CC)). F is 4 tensor order with ($Row_F \times COL_F \times$ Color channel (CC) $\times$ Color channel (CC)).In proposed CNN model, CC = 1 is selected for the input images.

$$Col_{row_{L+1},col_{L+1},CC'} = \sum_{row_L=0}^{row_L<Row_L} \sum_{Col_L=0}^{col_L<Col_L} \sum_{cc=0}^{cc<CC} F_{row_L,Col_L,cc,cc'} \otimes Input_{row_{L+1}+Row_L,Col_{L+1}+Col_{L,cc}} \quad (4)$$

Here in eq. (4) row_L, col_L, cc and cc' denote the indexing variables and L + 1 indicates next layer. The tensor 3 convolution input with tensor 4 order kernels creates $(Row_L - Row_F + 1) \times (Col_L - Col_F + 1) \times CC'$. Hyper parameter zero padding (adding columns/ rows containing 0 values) is utilized to obtain the desired input/output images in similar dimension. $\lfloor \frac{Row_L - 1}{2} \rfloor \lfloor \frac{Col_L - 1}{2} \rfloor$ denotes above row/ column padding and $\lfloor \frac{Row_L}{2} \rfloor, \lfloor \frac{Col_L}{2} \rfloor$ represents below row/column to obtain feature vectors having number of similar rows. Stride (s) is used to minimize the size of input. Pooling is applied to down sample the input vectors through minimizing spatial resolution. Max pooling utilized in the proposed model can be defined as in eq. (5).

$$Pooling_i = \underset{3 \tilde{n} 3}{max} Input_i^{3\times3} \quad (5)$$

Classification

In this phase, i_{th} feature vector is obtained with different kernel size through Alex/ Google CNN model. Then fully connected

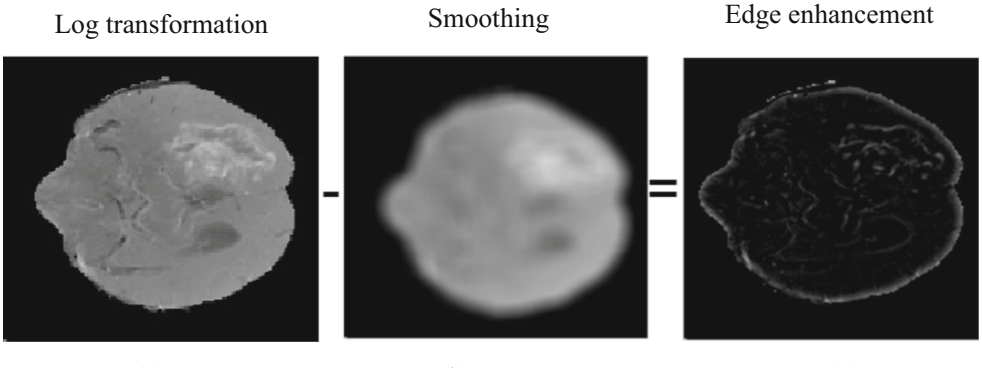

Fig. 3 Edge enhancement (Log transformation)

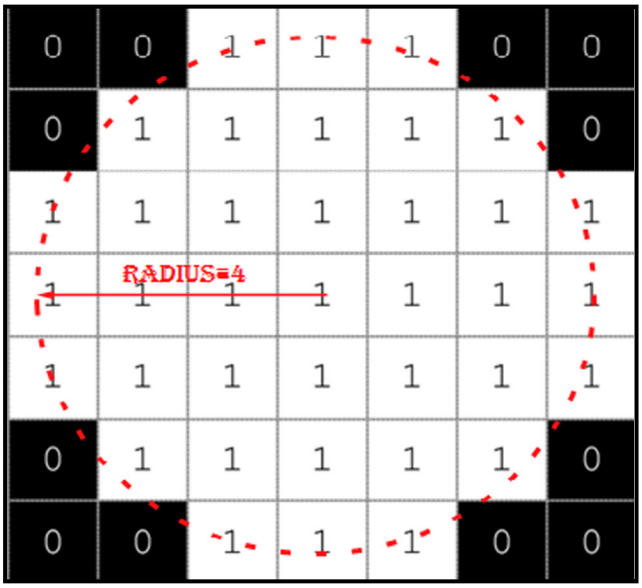

Fig. 4 Disk shape structuring element

and drop out layer is utilized to minimize over fitting problem. ReLU layer is used to enhance the characteristic of non-linear decision function. Equation (6) presents this.

$$f(Input) = \max(0, 1) \tag{6}$$

Here F_{Input} denotes related kernel vector of i_{th} neuron. Moreover, softmax and multiple classifiers are utilized for classification. Softmax layer performs classification on the basis of probability. In this layer, $\beta(Input_i)$ represents i_{th} class probability. The predicted class consists of high probability. N shows number of classes used for discrimination as given in eq. (7).

$$\beta(Input_i) = \frac{e^{F_i Input_i}}{\sum_{j=1}^{N} e^{F_i Input_i}} \tag{7}$$

The score vectors are obtained on softmax layer that provide prediction between the benign and malignant tumor. Moreover, both score vectors are fused and supplied to softmax [34] along with multiple selected classifiers (decision tree (DT), ensemble bagged (EB) tree [35], linear/ quadratic discriminant analysis (LDA) and linear/ quadratic support vector machine (SVM)) [36–40]) for prediction among tumor grades as shown in Fig. 8.

Results and discussion

Five benchmark datasets are processed to evaluate the brain data using MRI [41–43]. In BRATS 2013, 20 (HGG/ LGG) volumes are included in training and 10 in testing. BRATS 2014 contains 300 (HGG/ LGG) volumes where 200 volumes are utilized in training and 100 in testing. BRATS 2015 is having 220 HGG, 54 LGG

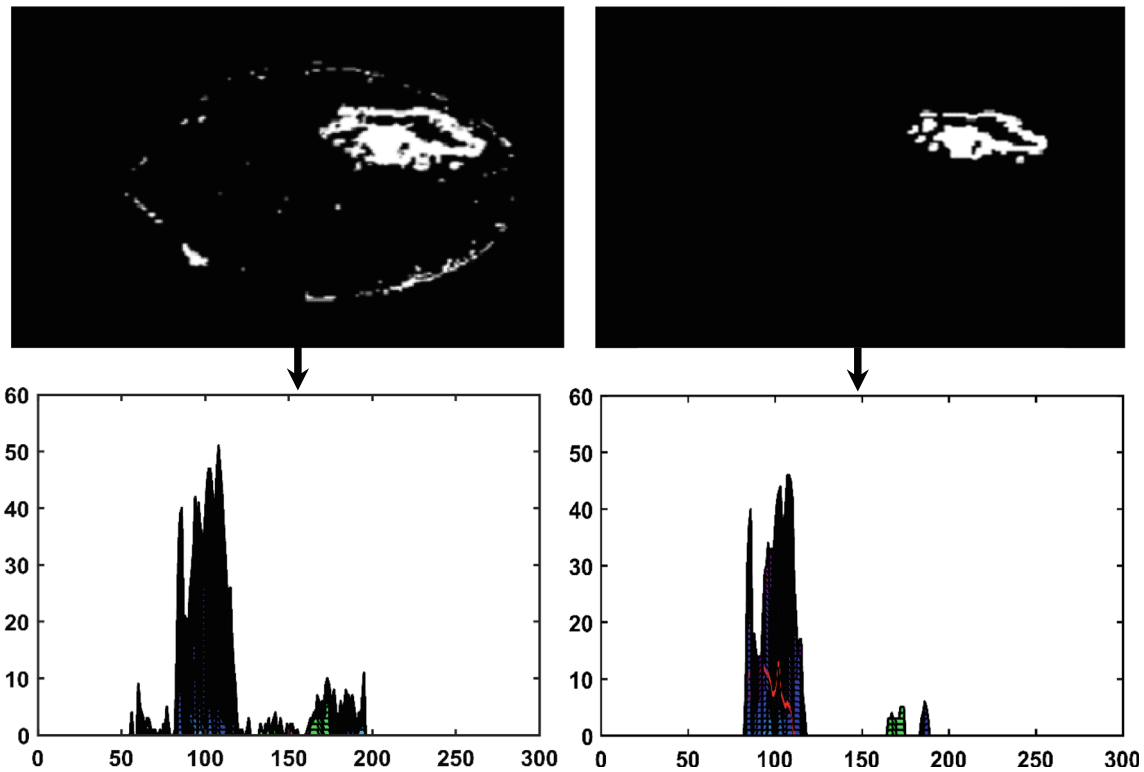

Fig. 5 Segmentation results (a) global threshold (b) morphological erosion

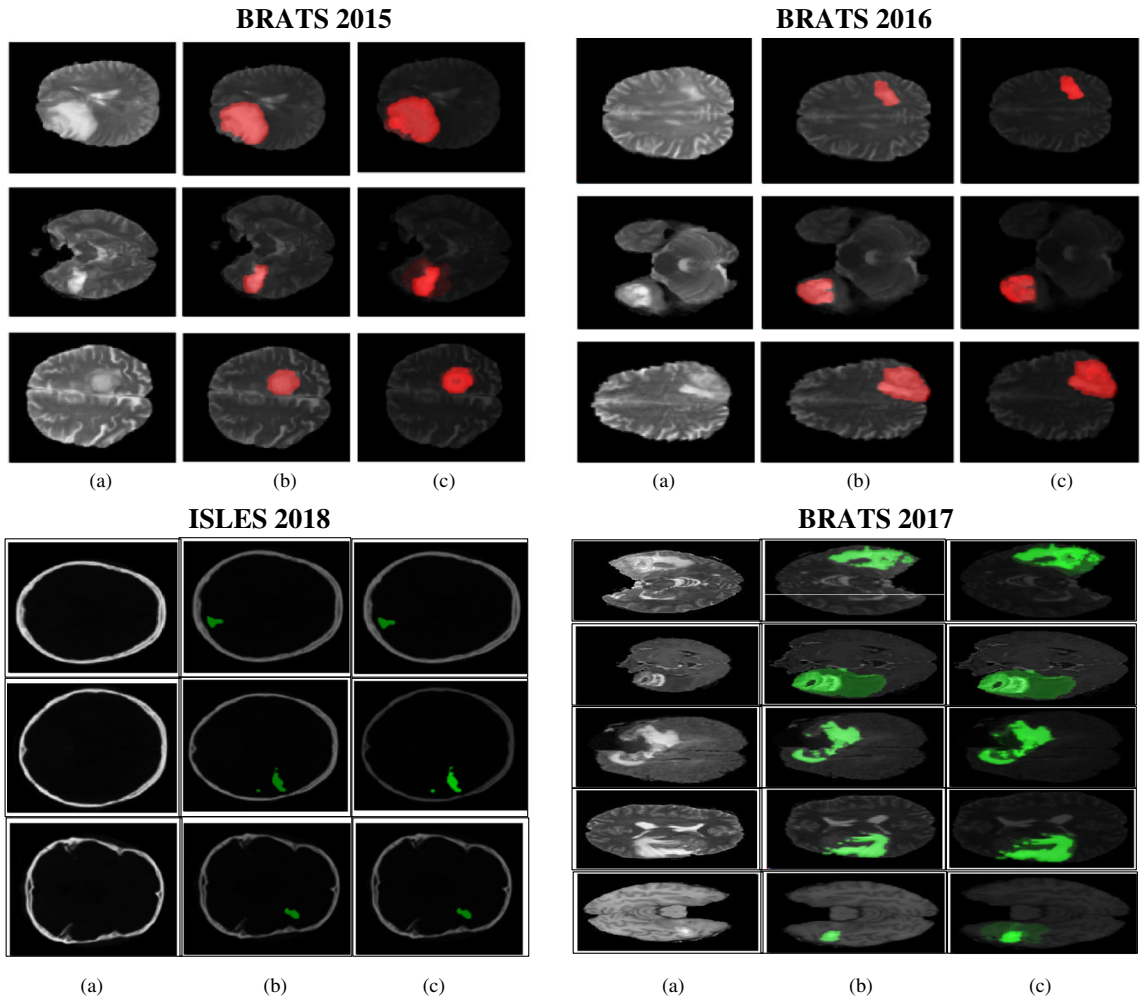

Fig. 6 Proposed method segmentation on benchmark datasets (a) input image (b) segmentation (c) ground truth

volumes in training and likewise 110 in testing. BRATS 2016 shares similar training database with BRATS 2015. BRATS 2017 contains 210 HGG and 75 LGG cases. ISLES 2018 has 63 patients' cases of CT having diffusion weighted imaging (DWI), cerebral blood volume (CBV) and cerebral blood flow (CBF) modalities in training and 40 testing cases. The BRATS dataset has three views of MRI i.e., axial, coronal and sagittal. The axial view divides the brain into superior (top) and inferior (bottom) parts. The sagittal view divides the brain into right and left halves and the coronal view into front and back (also known as dorsal, posterior or ventral and the anterior). The axial, sagittal and coronial views of brain are shown in Fig. 9.

In BRATS datasets, input slices are given in the form of MHA files. Therefore in this research work, axial view of brain slices are extracted using mha_read_header, mha_read_volume Matlab code (https://www.mathworks.com/matlabcentral/fileexchange/29344-read-medical-data-3d?focused=5186778&tab=function) and 3D slices are converted into 2D slices by using mat2gray Matlab command. The proposed model is trained on axial view for brain tumor segmentation and classification because this plane provides information related to top and bottom brain parts. However, when the proposed method is trained on coronial and sagittal views, it provides better results as well. Hence, brain tumor can be detected by the algorithm irrespective of view.

Image datasets description

The overall experiment is conducted on Intel Core I7 3.4 GHz, RAM 16.0 GB, 64-bit operating system (OS), ×64 based processor with NIVIDIA GeForce GTX 1080 GPU. The description of benchmark datasets is mentioned in Table 1.

The presented approach performance is evaluated in terms of dice similarity coefficient (DSC), accuracy (ACC), specificity (SP), sensitivity (SE) and area under the curve (AUC) as well as confusion matrix is shown in Fig. 10. The hyper parameters utilized for CNN training are reported in Table 2. The proposed methods running time is mentioned in Table 3.

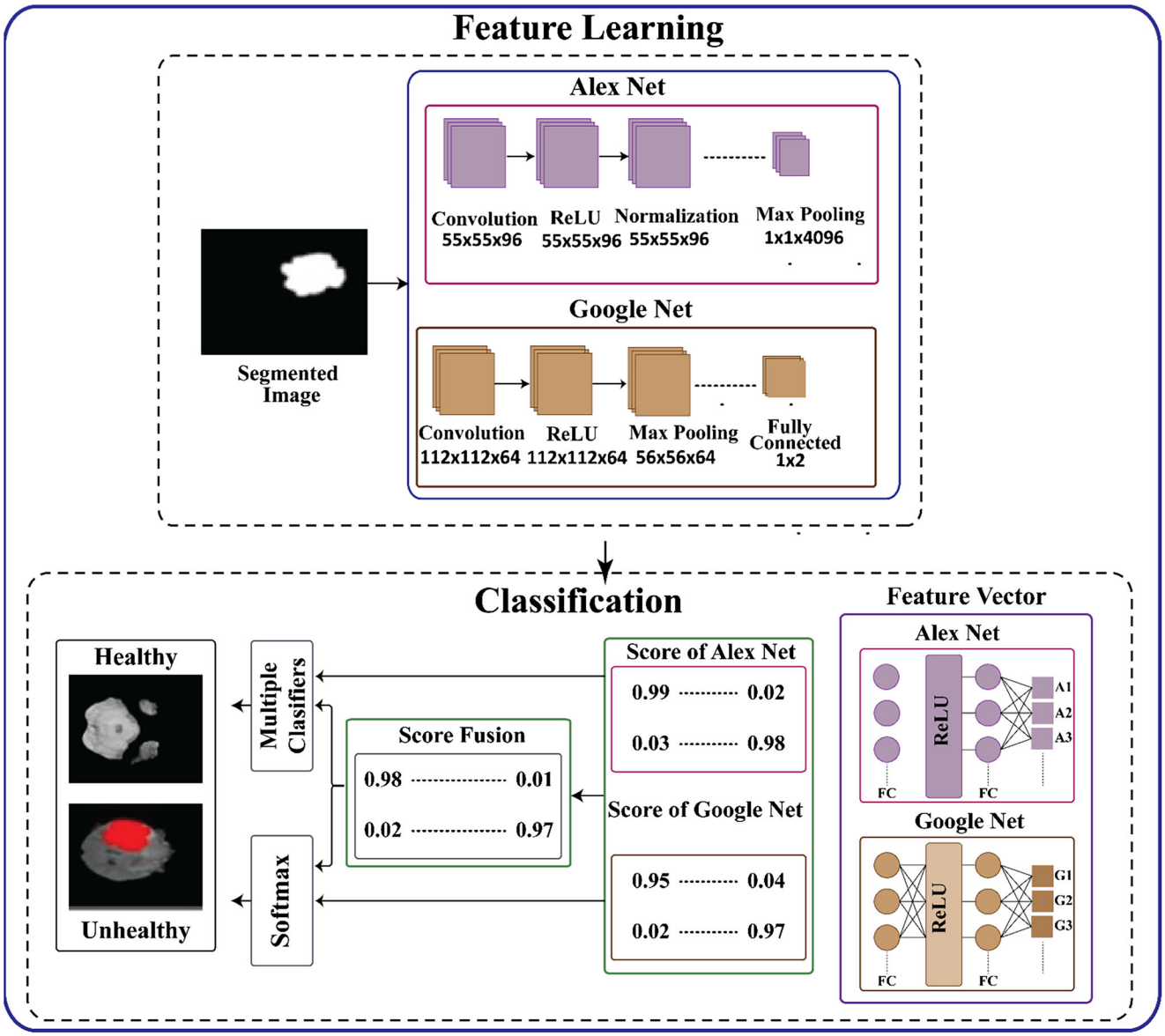

Fig. 7 Brain tumor classification using deep features

The evaluation of presented approach performance is measured on deep features fusion as well as individual features. Final results prove that feature fusion performs better as compared to individual features. The presented method results using Alex and Google are reported in Tables 4, 5, 6, 7 and 8. The graphical representation of suggested training results with respect to loss rate is shown in Fig. 11.

Fig. 8 Score based fusion

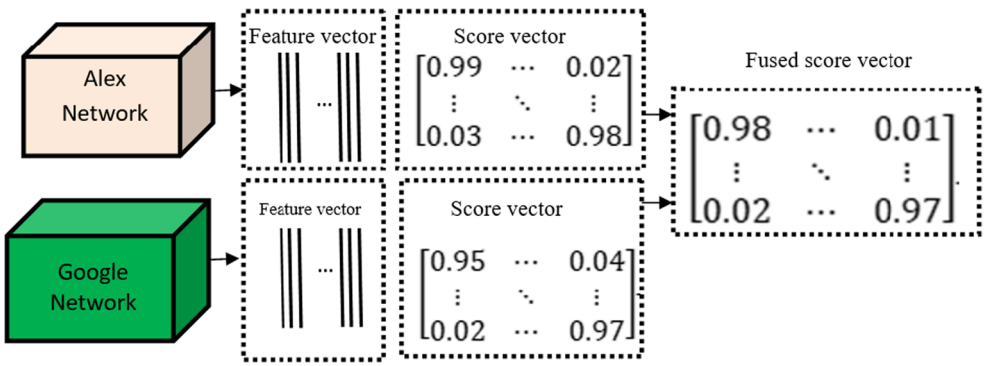

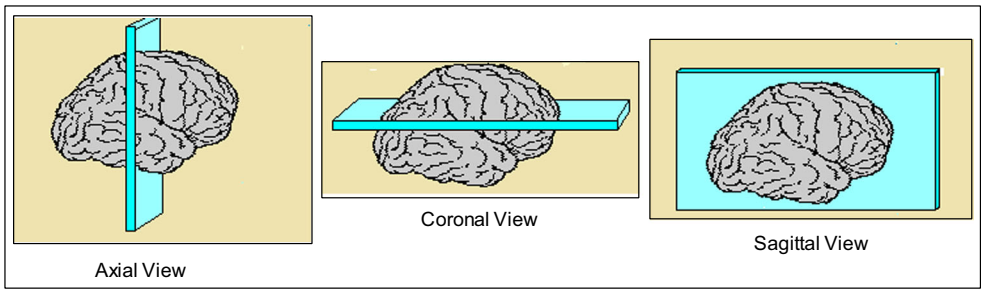

Fig. 9 Different views of brain https://www.faculty.washington.edu/chudler/slice.html

Table 1 Description of datasets used in proposed method

Datasets	Sequences	Cases/Volume	Dimension	High and low grade images	Normal and Glioma images (slices) used in this work (approx.)
BRATS 2013 Challenge	Flair, T1, T1C and T2	30 HGG and LGG	240 × 240 × 155 × 4 (155 slices in each case)	18,600 LGG and HGG	13,432 non-glioma and 4004 glioma images
BRATS 2014 Challenge		300 HGG and LGG	4 represents the number of sequences	186,000 LGG and HGG	61,920 non-glioma and 96,960 glioma images
BRATS 2015 Challenge		54 LGG, 220 HGG in training and 110 both HGG and LGG in testing		33,480 LGG, 136400 HGG in training and 68,200 both HGG and LGG in testing	15,456 non-glioma and 16,564 glioma images in training and 16,544 glioma and 7636 non-glioma images
BRATS 2017 Challenge		210 HGG, 75 LGG		46,500 LGG, 130200 HGG	19,032 non-glioma and 15,272 glioma images
ISLES 2018	DWI, CBV and CBF	94 cases	256 × 256 × 8 × 3 (8 slices in each case) 3 denotes number of sequences	2256 images	1800 stroke and 363 non-stroke images
BRATS 2016 Challenge	54 LGG, 220 HGG are included in training and testing cases are not given.				

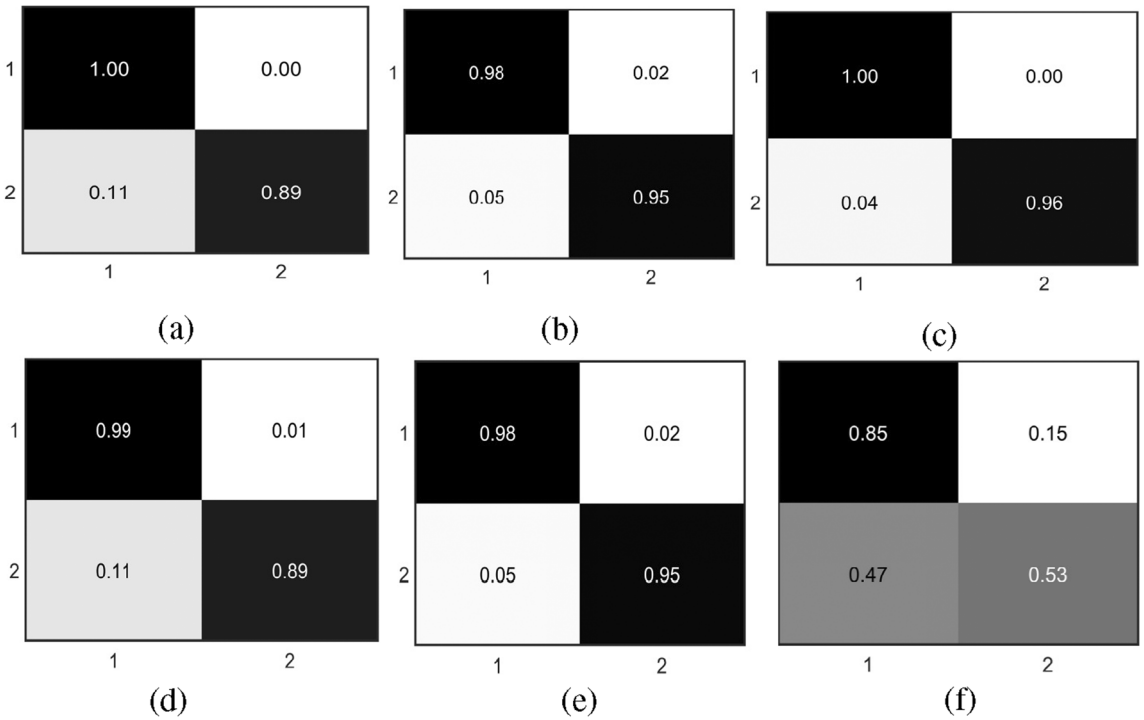

Fig. 10 Confusion matrices from each benchmark dataset (a) BRATS 2013 challenge (b) BRATS 2014 (c) BRATS 2015 challenge (d) BRATS 2016 (e) BRATS 2017 challenge (f) ISLES 2018

Table 2 Hyper parameters for proposed CNN model

Maximum Epochs	Size of Mini-Batch	Frequency of Validation	Validation of Patience	Initial Learning Rate
40	10	1	Inf	1e-4

Table 3 Running time of suggested approach

Proposed technique steps	Computational time (elapsed time)
Gray scale conversion	0.1822 Seconds
Contrast enhancement	1.7204 Seconds
Segmentation	32.4093 Seconds
Feature extraction (training)	542 Min and 49 Seconds
Parallel feature fusion and Optimal feature selection	3.1850 Seconds
Neural Network recognition (testing)	16.300 Seconds

Table 4 Presented method outcomes on benchmark datasets using Alex net scores

Dataset	ACC%	SP%	SE%	DSC	JSI	FPR	FNR	PPV%
BRATS 2013	0.9295	0.8824	0.9668	0.9387	0.8845	0.1176	0.0332	0.9122
BRATS 2014	0.8908	0.8929	0.8894	0.9069	0.8296	0.1071	0.1106	0.9250
BRATS 2015	0.9891	0.9820	0.9905	0.9934	0.9868	0.0180	0.0095	0.9962
BRATS 2016	0.9307	0.9919	0.8966	0.9430	0.8922	0.0081	0.1034	0.9945
BRATS 2017	0.9990	0.9989	1.0000	0.9942	0.9885	0.0011	0.0000	0.9885
ISLES 2018	0.7227	0.5862	0.7667	0.8070	0.6765	0.4138	0.2333	0.8519

Table 5 Presented method outcomes on benchmark datasets using Google net scores

Dataset	ACC%	SP%	SE%	DSC	JSI	FPR	FNR	PPV%
BRATS 2013	0.9278	0.8824	0.9636	0.9372	0.8818	0.1176	0.0364	0.9122
BRATS 2014	0.8879	0.8435	0.9204	0.9046	0.8259	0.1565	0.0796	0.8894
BRATS 2015	0.9801	0;.9561	0.9962	0.9934	0.9868	0.0439	0.0038	0.9905
BRATS 2016	0.9297	0.9764	0.9000	0.9399	0.8867	0.0236	0.1000	0.9836
BRATS 2017	0.9938	0.9966	0.9663	0.9663	0.9348	0.0034	0.0337	0.9663
ISLES 2018	0.7479	0.6250	0.7931	0.8214	0.6970	0.3750	0.2069	0.8519

Table 6 Presented method outcomes on benchmark datasets using fusion of Alex and Google net scores

Dataset	ACC%	SP%	SE%	DSC	JSI	FPR	FNR	PPV%
BRATS 2013	0.9666	0.9436	1.00	0.9607	0.9244	0.0564	0.00	0.9244
BRATS 2014	0.8966	0.9000	0.8942	0.9118	0.8378	0.1000	0.1058	0.9300
BRATS 2015	0.9984	1.00	0.9910	0.9955	0.9910	0.00	0.0090	1.00
BRATS 2016	0.9909	0.9945	0.9862	0.9896	0.9795	0.0055	0.0138	0.9931
BRATS 2017	0.9939	0.9892	1.00	0.9930	0.9861	0.0108	0.00	0.9861
ISLES 2018	0.7568	0.6380	0.8001	0.8318	0.6979	0.3641	0.2000	0.8620

Table 7 Proposed method performance using single feature vector of Alex network

Method		ACC%	SP%	SE%	DSC	JSI	FPR	FNR	PPV%
Ensemble	**BRATS 2013**	0.4608	0.5016	0.4120	0.4104	0.2582	0.4984	0.5880	0.4089
KNN		1.00	1.00	1.00	1.00	1.00	0.00	0.00	1.00
LDA		1.00	1.00	1.00	1.00	1.00	0.00	0.00	1.00
NB		0.9945	0.9869	1.00	0.9953	0.9906	0.0131	0.00	0.9906
SVM		1.00	1.00	1.00	1.00	1.00	0.00	0.00	1.00
DT		1.00	1.00	1.00	1.00	1.00	0.00	0.00	1.00
Logistic Regression		1.00	1.00	1.00	1.00	1.00	0.00	0.00	1.00
Ensemble	**BRATS 2014**	0.0196	0.00	1.00	0.0385	0.0196	1.00	0.00	0.0196
KNN		1.00	1.00	1.00	1.00	1.00	0.00	0.00	1.00
LDA		0.9862	1.00	0.5652	0.7222	0.5652	0.00	0.4348	1.00
NB		0.9856	0.9655	1.00	0.9878	0.9760	0.0345	0.00	0.9760
SVM		0.9858	0.9655	1.00	0.9881	0.9765	0.0345	0.00	0.9765
DT		1.00	1.00	1.00	1.00	1.00	0.00	0.00	1.00
Logistic Regression		1.00	1.00	1.00	1.00	1.00	0.00	0.00	1.00
Ensemble	**BRATS 2015**	0.5015	0.5023	0.5000	0.3985	0.2488	0.4977	0.5000	0.3313
KNN		1.00	1.00	1.00	1.00	1.00	0.000	0.00	1.00
LDA		0.9969	0.9908	1	0.9977	0.9954	0.0092	0.00	0.9954
NB		1.00	1.00	1.00	1.00	1.00	0.00	0.00	1.00
SVM		1.00	1.00	1.00	1.00	1.00	0.00	0.00	1.00
DT		1.00	1.00	1.00	1.00	1.00	0.00	0.00	1.00
Logistic Regression		1.00	1.00	1.00	1.00	1.00	0.00	0.00	1.00
Ensemble	**BRATS 2016**	0.8073	0.9951	0.5000	0.6631	0.4960	0.0049	0.5000	0.9841
KNN		1.00	1.00	1.00	1.00	1.00	0.00	0.00	1.00
LDA		0.9908	0.9764	1.00	0.9926	0.9852	0.0236	0.000	0.9852
NB		0.9847	0.9760	0.9901	0.9877	0.9756	0.0240	0.0099	0.9852
SVM		0.9878	0.9852	0.9919	0.9840	0.9685	0.0148	0.0081	0.9762
DT		0.9939	0.9901	1.00	0.9920	0.9841	0.0099	0.00	0.9841
Logistic Regression		0.9847	0.9901	0.9760	0.9799	0.9606	0.0099	0.0240	0.9839
Ensemble	**BRATS 2017**	0.8012	1.00	0.4758	0.6448	0.4758	0.00	0.5242	1.00
KNN		1.00	1.00	1.00	1.00	1.00	0.00	0.00	1.00
LDA		0.9730	0.9852	0.9538	0.9650	0.9323	0.0148	0.0462	0.9764
NB		0.9848	0.9852	0.9841	0.9802	0.9612	0.0148	0.0159	0.9764
SVM		0.9878	0.9852	0.9919	0.9840	0.9685	0.0148	0.0081	0.9762
DT		0.9939	0.9841	1.00	0.9950	0.9901	0.0159	0.00	0.9901
Logistic Regression		0.9847	0.9839	0.9852	0.9877	0.9756	0.0161	0.0148	0.9901
Ensemble	**ISLES 2018**	0.9914	0.9913	0.9920	0.9484	0.9019	0.0087	0.0080	0.9086
KNN		0.9971	1.00	0.9651	0.9651	0.9822	0.00	0.0349	1.00
LDA		0.9972	0.9991	0.9703	0.9790	0.9589	8.6690	0.0297	0.9879
NB		0.9946	0.9996	0.9433	0.9686	0.9391	4.3528	0.0567	0.9953
SVM		0.9880	0.9888	0.9669	0.8643	0.7611	0.0112	0.0331	0.7814
DT		0.9920	0.9929	0.9639	0.8797	0.7852	0.0071	0.0361	0.8091
Logistic Regression		0.9893	0.9894	0.9877	0.9407	0.8880	0.0106	0.0123	0.8979

Table 8 Proposed method performance using single feature vector of Google network

Method		ACC%	SP%	SE%	DSC	JSI	FPR	FNR	PPV%
Ensemble	**BRATS 2013**	0.7607	0.9687	0.4591	0.6103	0.4391	0.0313	0.5409	0.9099
KNN		0.9963	1.00	0.9910	0.9955	0.9910	0.00	0.0090	1.00
LDA		0.9295	0.8824	0.9668	0.9387	0.8845	0.1176	0.0332	0.9122
NB		0.9276	0.9636	0.8819	0.9147	0.8427	0.0364	0.1181	0.9500
SVM		0.9276	0.9605	0.8851	0.9143	0.8421	0.0395	0.1149	0.9455
DT		0.9722	0.9935	0.9437	0.9667	0.9356	0.0065	0.0563	0.9909
Logistic Regression		0.9177	0.9145	0.9211	0.9170	0.8468	0.0855	0.0789	0.9130
Ensemble	**BRATS 2014**	0.8591	0.6778	0.9375	0.9028	0.8228	0.3222	0.0625	0.8705
KNN		0.9971	1.00	0.9929	0.9964	0.9929	0.00	0.0071	1.00
LDA		0.8908	0.9250	0.8446	0.8681	0.7669	0.0750	0.1554	0.8929
NB		0.9295	0.8824	0.9668	0.9387	0.8845	0.1176	0.0332	0.9122
SVM		0.8879	0.8857	0.8894	0.9046	0.8259	0.1143	0.1106	0.9204
DT		0.9569	0.9286	0.9760	0.9644	0.9312	0.0714	0.0240	0.9531
Logistic Regression		0.8908	0.8446	0.9250	0.9069	0.8296	0.1554	0.0750	0.8894
Ensemble	**BRATS 2015**	0.5015	0.5023	0.5000	0.3985	0.2488	0.4977	0.5000	0.3313
KNN		0.9970	0.9908	1.00	0.9977	0.9955	0.0092	0.00	0.9955
LDA		0.9969	0.9908	1.00	0.9977	0.9954	0.0092	0.00	0.9954
NB		0.9969	0.9908	1.00	0.9977	0.9954	0.0092	0.00	0.9954
SVM		1.00	1.00	1.00	1.00	1.00	0.00	0.00	1.00
DT		1.00	1.00	1.00	1.00	1.00	0.00	0.00	1.00
Logistic Regression		1.00	1.00	1.00	1.00	1.00	0.00	0.00	1.00
Ensemble	**BRATS 2016**	0.7645	0.9606	0.4435	0.5882	0.4167	0.0394	0.5565	0.8730
KNN		1.00	1.00	1.00	1.00	1.00	0.00	0.00	1.00
LDA		0.9327	0.8966	0.9919	0.9179	0.8483	0.1034	0.0081	0.8542
NB		0.9327	0.8966	0.9919	0.9179	0.8483	0.1034	0.0081	0.8542
SVM		0.9327	0.8966	0.9919	0.9179	0.8483	0.1034	0.0081	0.8542
DT		0.9694	0.9606	0.9839	0.9606	0.9242	0.0394	0.0161	0.9385
Logistic Regression		0.9327	0.9919	0.8966	0.9430	0.8922	0.0081	0.1034	0.9945
Ensemble	**BRATS 2017**	0.7615	0.9606	0.4355	0.5806	0.4091	0.0394	0.5645	0.8710
KNN		1.00	1.00	1.00	1.00	1.00	0.00	0.00	1.00
LDA		0.9327	0.8542	0.9945	0.9430	0.8922	0.1458	0.0055	0.8966
NB		0.9031	0.5227	0.9945	0.9430	0.8922	0.4773	0.0055	0.8966
SVM		0.9327	0.8542	0.9945	0.9430	0.8922	0.1458	0.0055	0.8966
DT		0.9694	0.9606	0.9839	0.9606	0.9242	0.0394	0.0161	0.9385
Logistic Regression		0.9903	0.9945	0.9840	0.9880	0.9762	0.0055	0.0160	0.9919
Ensemble	**ISLES 2018**	0.9977	1.00	0.9578	0.9785	0.9578	0.0000	0.0422	1.000
KNN		0.9991	1.00	0.9669	0.9832	0.9669	0.0331	0.00	1.00
LDA		1.00	1.00	0.9578	0.9785	0.9578	0.00	0.0422	1.00
NB		0.9881	0.9892	0.9626	0.8693	0.7688	0.0108	0.0374	0.7925
SVM		0.9821	0.9823	0.9760	0.5946	0.5946	0.0177	0.0240	0.6034
DT		0.9984	0.9994	0.9833	0.9870	0.9744	6.2528	0.0167	0.9907
Logistic Regression		0.9977	0.9993	0.9776	0.9846	0.9697	6.5220	0.0224	0.9917

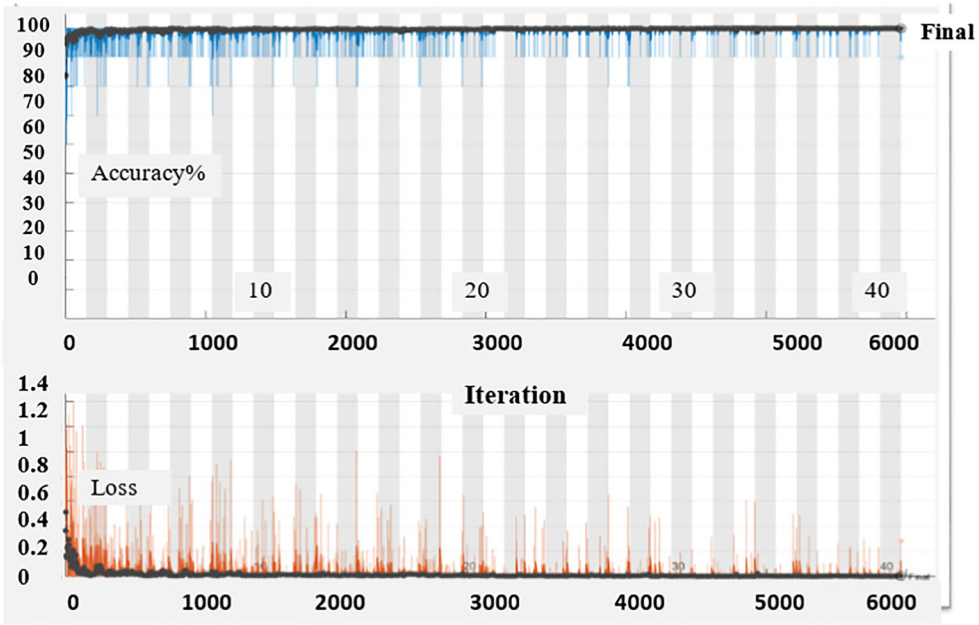

Fig. 11 Training results with respect to loss rate

BRATS 2015 achieves maximum (0.9891) ACC using Alex net and ISLES 2018 obtains 0.7479 ACC using Google net. The experimental results on fusion of both Alex and Google feature vectors are mentioned in Table 9.

Relative operating characteristic (ROC) curve and confusion matrix across each dataset are shown in Fig. 12. Finally, it is concluded that k nearest neighbor (KNN) performs better. The suggested approach results are compared with existing techniques in Table 10 where it is identified that proposed method outperforms as compared with existing approaches.

Conclusion and discussion

This study presents a new score level fusion technique. The proposed approach achieves better results on MRI/ CT images. The presented method is evaluated on individual score vectors as well as both score vectors of pre-trained CNN models are fused on the basis of different performance measures as 0.9667 ACC (fused score vector), 0.9295 ACC (Alex net), 0.9278 ACC (Google net) on BRATS 2013, 0.9971 ACC (fusion of Alex and Google), 0.8908 ACC (Alex net), 0.8879 ACC (Google net) on BRATS 2014, 0.9938 ACC (fusion of Alex and Google), 0.9891 ACC (Alex), 0.9801ACC (Google net) on BRATS 2015, 1.00ACC (fusion of Alex and Google), 0.9307 ACC (Alex net), 0.9297 ACC (Google net), 0.9971 ACC (fusion of Alex and Google), 0.7227 (Alex net), 0.7479 (Google net) on ISLES 2018 datasets respectively. The achieved results are compared with existing techniques that proves the novelty of suggested method. The proposed score based fusion method is light weight and accurately segments/classifies only complete

Table 9 Proposed method performance using fused feature vector of Alex and Google nets

Method		ACC%	SP%	SE%	DSC	JSI	FPR	FNR	PPV%
Ensemble	**BRATS 2013**	0.9283	0.9358	0.9171	0.9108	0.8361	0.0642	0.0829	0.9045
KNN		0.9963	1.00	0.9937	0.9969	0.9937	0.0063	0.00	1.00
LDA		0.9667	1.00	0.9542	0.9766	0.9542	0.00	0.0458	1.00
NB		0.9587	0.9429	0.9651	0.9708	0.9432	0.0571	0.0349	0.9765
SVM		0.9276	0.8851	0.9605	0.9374	0.8822	0.1149	0.0395	0.9154
DT		0.9722	0.9437	0.9935	0.9761	0.9533	0.0563	0.0065	0.9592
Logistic Regression		0.9684	0.9505	0.9762	0.9774	0.9557	0.0495	0.0238	0.9785
Ensemble	**BRATS 2014**	0.9260	0.9231	0.9279	0.9392	0.8853	0.0769	0.0721	0.9507
KNN		0.9971	1.00	0.9952	0.9976	0.9952	0.000	0.0048	1.00
LDA		0.9659	0.9467	0.9743	0.9755	0.9523	0.0533	0.0257	0.9768
NB		0.9664	0.9444	0.9766	0.9754	0.9519	0.0556	0.0234	0.9741
SVM		0.9569	0.9630	0.9531	0.9644	0.9312	0.0370	0.0469	0.9760
DT		0.8879	0.8435	0.9204	0.9046	0.8259	0.1565	0.0796	0.8894
Logistic Regression		0.9302	0.8854	0.9512	0.9489	0.9028	0.1146	0.0488	0.9466
Ensemble	**BRATS 2015**	0.9847	0.9832	1.00	0.9244	0.8594	0.0168	0.00	0.8594
KNN		0.9938	1.00	0.9649	0.9821	0.9649	0.00	0.0351	1.00
LDA		0.9906	0.9910	0.9905	0.9943	0.9887	0.0090	0.0095	0.9981
NB		0.9891	0.9909	0.9887	0.9934	0.9868	0.0091	0.0113	0.9981
SVM		0.9906	0.9561	0.9981	0.9943	0.9887	0.0439	0.0019	0.9906
DT		0.9938	0.9737	0.9981	0.9962	0.9924	0.0263	0.0019	0.9943
Logistic Regression		0.9891	0.9820	0.9905	0.9934	0.9868	0.0180	0.0095	0.9962
Ensemble	**BRATS 2016**	0.9541	0.9653	0.9360	0.9398	0.8864	0.0347	0.0640	0.9435
KNN		1.00	1.00	1.00	1.00	1.00	0.00	0.00	1.00
LDA		0.9327	0.8542	0.9945	0.9430	0.8922	0.1458	0.0055	0.8966
NB		0.9419	0.9921	0.9104	0.9506	0.9059	0.0079	0.0896	0.9946
SVM		0.9480	0.9921	0.9204	0.9561	0.9158	0.0079	0.0796	0.9946
DT		0.9694	0.9839	0.9606	0.9750	0.9512	0.0161	0.0394	0.9898
Logistic Regression		0.9327	0.9840	0.9010	0.9430	0.8922	0.0160	0.0990	0.9891
Ensemble	**BRATS 2017**	0.9944	0.9943	0.9946	0.9839	0.9683	0.0057	0.0054	0.9734
KNN		0.9972	0.9989	0.9891	0.9918	0.9838	0.0011	0.0109	0.9734
LDA		0.9838	0.9875	0.9713	0.9844	0.9692	0.0287	0.0125	0.9977
NB		0.9803	0.9711	0.9821	0.9882	0.9766	0.0289	0.0179	0.9943
SVM		0.9775	0.9819	0.9767	0.9865	0.9735	0.0181	0.0233	0.9966
DT		0.9906	0.9780	0.9932	0.9943	0.9888	0.0220	0.0068	0.9955
Logistic Regression		0.9991	0.9944	1.00	0.9994	0.9989	0.0056	0.000	0.9989
Ensemble	**ISLES 2018**	0.9260	0.9231	0.9279	0.9392	0.8853	0.0769	0.0721	0.9507
KNN		0.9971	1.00	0.9952	0.9976	0.9952	0.000	0.0048	1.00
LDA		0.9659	0.9467	0.9743	0.9755	0.9523	0.0533	0.0257	0.9768
NB		0.9664	0.9444	0.9766	0.9754	0.9519	0.0556	0.0234	0.9741
SVM		0.9569	0.9630	0.9531	0.9644	0.9312	0.0370	0.0469	0.9760
DT		0.8879	0.8435	0.9204	0.9046	0.8259	0.1565	0.0796	0.8894
Logistic Regression		0.9302	0.8854	0.9512	0.9489	0.9028	0.1146	0.0488	0.9466

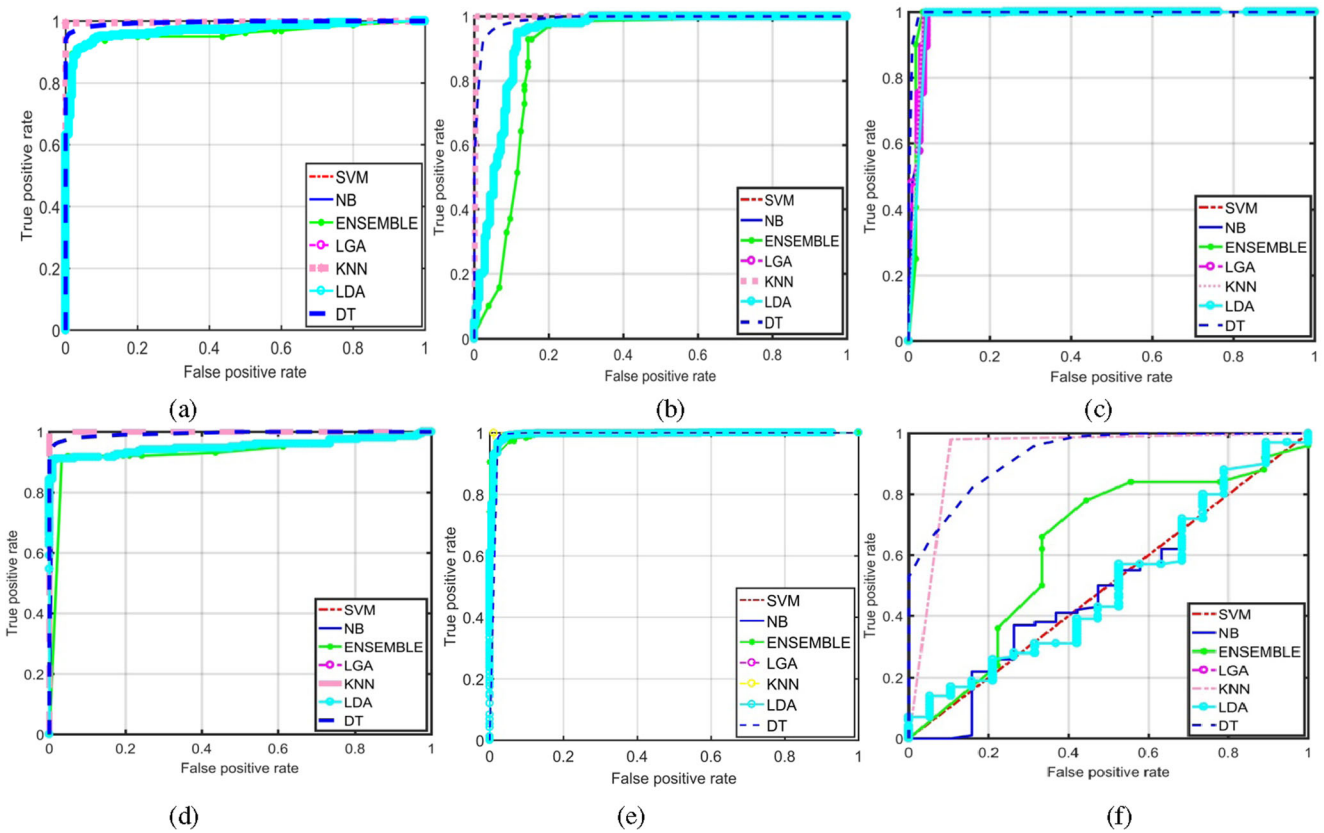

Fig. 12 ROC using benchmark challenge datasets (a) 2013 (b) 2014 (c) 2015 (d) 2016 (e) 2017 (f) 2018

Table 10 Proposed method comparison

Datasets	Year	Method	SE%	SP%	DSC	PPV%
BRATS 2013	2017	InputCascadeCNN [21]	0.87	0.89	0.88	–
	2018	FCNN +3D CRF (fusing) [44]	0.86		0.88	0.90
	2017	Deep Neural Networks (DNNs) [21]	0.85	–	0.85	0.85
	2019	[45]	–	–	0.81	–
	Proposed		**0.9762**	**0.9505**	**0.9774**	**0.9785**
BRATS 2014	2015	Texture feature [46]			89.6	
	Proposed		**0.9531**	**0.9630**	**0.9644**	**0.9760**
BRATS 2015	2017	Ensemble+CRF [24]	89.1	–	90.1	–
	2018	FCNN +3D CRF (fusing) [44]	0.82		0.84	0.89
	2019	[47]	–	–	–	0.83
	Proposed		**0.9905**	**0.9820**	**0.9962**	**0.9962**
BRATS 2016	2017	Iterative random forest [48]	0.84 ± 0.10	0.98 ± 0.01	0.81 ± 0.09	–
	Proposed		**0.9839**	**0.9606**	**0.9506**	**0.9898**
BRATS 2017	2017	FCNN [49]	–	–	0.83	–
	2017	3D U-Net [50]	0.9995	0.5014	0.1189	–
	2017	Recurrent neural networks [51]	0.818	–	0.864	0.941
	2019	[47]	–	–	–	0.87
	Proposed		**0.9944**	**1.00**	**0.9994**	**0.9989**

tumor region. In future, this research work might be enhanced to segment and classify the sub-tumoral region i.e., enhance, non-enhance and complete tumor respectively. Further, proposed work can be extended for brain tumor detection in coronial and saggital views.

Nomenclature ∇, Sharp edges; $\otimes$, Convolutional; ε, Smoothing; S_i, Resultant image; T , Threshold; $\mathcal{R}$, , Opening; λ, Erosion; Ψ, Dilation; L, Layer; F, Kernels bank; S, Stride; CC, Channel; Col, Column; $\beta(\text{Input}_i)$, Softmax; N, Number of layers; F_{Input}, Kernel vector of i_{th} neuron; e , Probability

References

1. Amin, J., Sharif, M., Yasmin, M., and Fernandes, S.L., A distinctive approach in brain tumor detection and classification using MRI. Pattern Recognition Letters, 2017.
2. Bauer, S., Wiest, R., Nolte, L.-P., Reyes, M.J., PiM, Biology. A survey of MRI-based medical image analysis for brain tumor studies. 58 (13):R97, 2013.
3. Rajinikanth, V., Satapathy, S. C., Fernandes, S. L., and Nachiappan, S., Entropy based segmentation of tumor from brain MR images–a study with teaching learning based optimization. *Pattern Recogn. Lett.* 94:87–95, 2017.
4. Upadhyay, N., and AJTBjor, W., Conventional MRI evaluation of gliomas. 84 (special_issue_2):S107-S111, 2011.
5. Nida, N., Sharif, M., Khan, M. U. G., Yasmin, M., and Fernandes, S. L., A framework for automatic colorization of medical imaging. *IIOAB J.* 7:202–209, 2016.
6. Gordillo, N., Montseny, E., and Sobrevilla, P.J., State of the art survey on MRI brain tumor segmentation. 31 (8):1426–1438, 2013.
7. Zhang, L., Song, M., Liu, X., Bu, J., and Chen, C.J.S.P., Fast multi-view segment graph kernel for object classification. 93 (6):1597–1607, 2013.
8. Adams, R., and Bischof, L.J., ITopa, intelligence m. Seeded region growing. 16 (6):641–647, 1994.
9. Han, J., Quan, R., Zhang, D., and Nie, F.J.I., ToIP Robust object co-segmentation using background prior. 27 (4):1639–1651, 2018.
10. Raja, N.S.M., Fernandes, S., Dey, N., Satapathy, S.C., and Rajinikanth, V., Contrast enhanced medical MRI evaluation using Tsallis entropy and region growing segmentation. Journal of Ambient Intelligence and Humanized Computing:1–12, 2018.
11. Rajinikanth, V., Fernandes, S.L., Bhushan, B., and Sunder, N.R., Segmentation and analysis of brain tumor using Tsallis entropy and regularised level set. Proceedings of 2nd international conference on micro-electronics, electromagnetics and telecommunications. Springer, 313–321, 2018.
12. Deng, W., Xiao, W., Deng, H., and Liu, J., MRI brain tumor segmentation with region growing method based on the gradients and variances along and inside of the boundary curve. Biomedical engineering and informatics (BMEI), 2010 3rd international conference on, IEEE. 393–396, 2010.
13. Zhang, L., Han, Y., Yang, Y., Song, M., Yan, S., and Tian, QJIToIP., Discovering discriminative graphlets for aerial image categories recognition. 22 (12):5071–5084, 2013.
14. Menze, B.H., Van Leemput, K., Lashkari, D., Weber, M.-A., Ayache, N., and Golland, P., A generative model for brain tumor segmentation in multi-modal images. International conference on medical image computing and computer-assisted intervention, Springer. 151–159, 2010.
15. Cheng, G., Zhou, P., and Han, JJIToIP., Duplex metric learning for image set classification. 27 (1):281–292, 2018.
16. Lee, C.-H., Wang, S., Murtha, A., Brown, M.R., and Greiner, R., Segmenting brain tumors using pseudo–conditional random fields. International conference on medical image computing and computer-assisted intervention. Springer. 359–366, 2008.
17. Zhang, C., Fang, M., and Nie, H., Brain tumor segmentation using fully convolutional networks from magnetic resonance imaging. *J. Med. Imag. Health Inform.* 8(8):1546–1553, 2018.
18. Ghosh, A., Maso, F.D., Roig, M., Mitsis, G.D., and Boudrias, M.-H., Deep semantic architecture with discriminative feature visualization for neuroimage analysis. arXiv preprint arXiv:180511704, 2018.
19. Zhao, L., and Jia K., Multiscale cnns for brain tumor segmentation and diagnosis. Computational and mathematical methods in medicine 2016.
20. Cui, Z., Yang, J., and Qiao, Y., Brain MRI segmentation with patch-based CNN approach. Control conference (CCC), 2016 35th Chinese. IEEE. 7026–7031, 2016.
21. Havaei, M., Davy, A., Warde-Farley, D., Biard, A., Courville, A., Bengio, Y., Pal, C., Jodoin, P.-M., and Larochelle, H., Brain tumor segmentation with deep neural networks. *Med. Image Anal.* 35:18–31, 2017.
22. Yamashita, R., Nishio, M., Do, R.K.G., and Togashi, K., Convolutional neural networks: An overview and application in radiology. Insights into imaging:1–19, 2018.
23. Abdel-Maksoud, E., Elmogy, M., and Al-Awadi, R., Brain tumor segmentation based on a hybrid clustering technique. *Egypt Inform. J.* 16(1):71–81, 2015.
24. Kamnitsas, K., Ledig, C., Newcombe, V. F., Simpson, J. P., Kane, A. D., Menon, D. K., Rueckert, D., and Glocker, B., Efficient multi-scale 3D CNN with fully connected CRF for accurate brain lesion segmentation. *Med. Image Analy.* 36:61–78, 2017.
25. Amin, J., Sharif, M., Yasmin, M., and Fernandes, S. L., Big data analysis for brain tumor detection: Deep convolutional neural networks. *Fut. Gen. Comput. Syst.* 87:290–297, 2018.
26. Dong, H., Yang, G., Liu, F., Mo, Y., Guo, Y., Automatic brain tumor detection and segmentation using U-net based fully convolutional networks. Annual conference on medical image understanding and analysis. Springer, 506–517, 2017.
27. Kamnitsas, K., Ferrante, E., Parisot, S., Ledig, C., Nori, A. V., Criminisi, A., Rueckert, D., and Glocker, B., DeepMedic for brain tumor segmentation. In: International workshop on Brainlesion: Glioma, multiple sclerosis, stroke and traumatic brain injuries. Springer, 2016, 138–149.
28. Bernal, J., Kushibar, K., Asfaw, D. S., Valverde, S., Oliver, A., Martí, R., and Lladó, X., Deep convolutional neural networks for brain image analysis on magnetic resonance imaging: A review. Artificial intelligence in medicine, 2018.
29. Isensee, F., Petersen, J., Klein, A., Zimmerer, D., Jaeger, P.F., Kohl, S., Wasserthal, J., Koehler, G., Norajitra, T., and Wirkert, S., Nnu-net: Self-adapting framework for u-net-based medical image segmentation. arXiv preprint arXiv:180910486, 2018.
30. Hai, J., Qiao, K., Chen, J., Tan, H., Xu, J., Zeng, L., Shi, D., and Yan, B., Fully Convolutional DenseNet with Multiscale Context for Automated Breast Tumor Segmentation. Journal of Healthcare Engineering, 2019.
31. Satapathy, S. C., Fernandes, S. L., and Lin, H., Stroke lesion segmentation and analysis using entropy/Otsu's function–a study with social group optimization. *Curr. Bioinform.* 14(4):305–313, 2019.
32. Alex, Krizhevsky., Sutskever, Ilya., and Hinton, GE., ImageNet Classification with Deep Convolutional Neural Networks. Advances in neural information processing systems, 2012.
33. Zhou, B., Khosla, A., Lapedriza, A., Torralba, A., and Oliva, A., Places: An image database for deep scene understanding, (2016).
34. Raza, M., Sharif, M., Yasmin, M., Khan, M. A., Saba, T., and Fernandes, S. L., Appearance based pedestrians' gender

recognition by employing stacked auto encoders in deep learning. *Fut. Gen. Comput. Syst.* 88:28–39, 2018.
35. Amin, J., Sharif, M., Yasmin, M., Ali, H., and Fernandes, S. L., A method for the detection and classification of diabetic retinopathy using structural predictors of bright lesions. *J. Comput. Sci.* 19:153–164, 2017.
36. Shah, J.H., Sharif, M., Yasmin, M., and Fernandes, S.L., Facial expressions classification and false label reduction using LDA and threefold SVM. Pattern Recognition Letters, 2017.
37. Sharif, M., Khan, M.A., Faisal, M., Yasmin, M., and Fernandes, S.L., A framework for offline signature verification system: Best features selection approach. Pattern Recognition Letters, 2018.
38. Liaqat, A., Khan, M. A., Shah, J. H., Sharif, M., Yasmin, M., and Fernandes, S. L., Automated ulcer and bleeding classification from WCE images using multiple features fusion and selection. *J. Mech. Med. Biol.* 18(04):1850038, 2018.
39. Ansari, G. J., Shah, J. H., Yasmin, M., Sharif, M., and Fernandes, S. L., A novel machine learning approach for scene text extraction. *Fut. Gen. Comput. Syst.* 87:328–340, 2018.
40. Naqi, S., Sharif, M., Yasmin, M., and Fernandes, S. L., Lung nodule detection using polygon approximation and hybrid features from CT images. *Curr. Med. Imag. Rev.* 14(1):108–117, 2018.
41. Menze, B. H., Jakab, A., Bauer, S., Kalpathy-Cramer, J., Farahani, K., Kirby, J., Burren, Y., Porz, N., Slotboom, J., and Wiest, R., The multimodal brain tumor image segmentation benchmark (BRATS). *IEEE Trans. Med. Imag.* 34(10):1993, 2015.
42. Kistler, M., Bonaretti, S., Pfahrer, M., Niklaus, R., and Büchler, P., The virtual skeleton database: An open access repository for biomedical research and collaboration. Journal of medical Internet research 15 (11), 2013.
43. Maier, O., Menze, B. H., von der Gablentz, J., Häni, L., Heinrich, M. P., Liebrand, M., Winzeck, S., Basit, A., Bentley, P., and Chen, L., ISLES 2015-a public evaluation benchmark for ischemic stroke lesion segmentation from multispectral MRI. *Med. Image Analy.* 35:250–269, 2017.
44. Zhao, X., Wu, Y., Song, G., Li, Z., Zhang, Y., and Fan, Y., A deep learning model integrating FCNNs and CRFs for brain tumor segmentation. Med. Image Analy. 43:98–111, 2018.
45. Bhagat, P., and Choudhary, P., Multiclass segmentation of brain tumor from MRI images. In: Applications of artificial intelligence techniques in engineering. Springer, 543–553, 2019.
46. Reza, S.M., and Mays, R., Iftekharuddin KM multi-fractal detrended texture feature for brain tumor classification. Proceedings of SPIE–the International Society for Optical Engineering. NIH Public Access, 2015.
47. Chen, S., Ding, C., and Liu, M., Dual-force convolutional neural networks for accurate brain tumor segmentation. *Pattern Recogn.* 88:90–100, 2019.
48. Ellwaa, A., Hussein, A., AlNaggar, E., Zidan, M., Zaki, M., Ismail, M.A., and Ghanem, N.M., Brain tumor segmantation using random forest trained on iteratively selected patients. International workshop on Brainlesion: Glioma, multiple sclerosis, stroke and traumatic brain injuries. Springer, 129–137, 2016.
49. Van Der Kouwe, A., Brain tumor segmentation from multi modal MR images using fully convolutional neural network. Proceedings of the 6th MICCAI BraTS challenge, 2017.
50. Amorim, P.H.A.C.V.S., Escudero, G.G., Oliveira, D.D.C., Pereira, S.M., Santos, H.M., and Scussel, A.A., 3D U-nets for brain tumor segmentation in MICCAI 2017 BraTS challenge proceedings of the 6th MICCAI BraTS Challenge, 2017.
51. Simon Andermatt, S.P., and Cattin, P., Multi-dimensional gated recurrent units for brain tumor segmentation. Proceedings of the 6th MICCAI BraTS Challenge (2017), 1984.